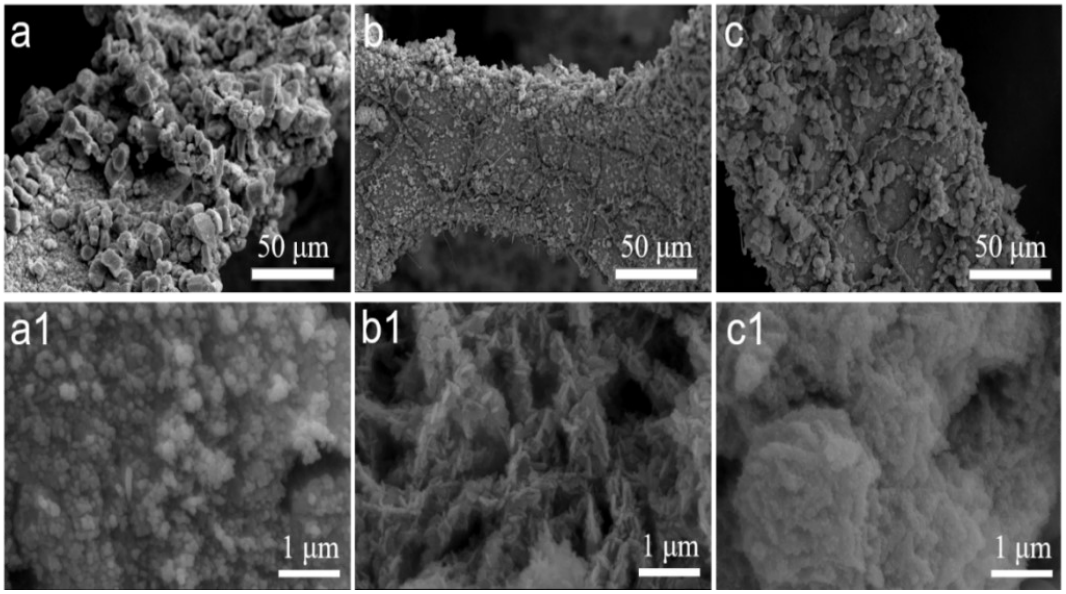

Fig. S1. (a)W-CoSe200/NF， (b) W-CoSe300/NF， (c) W-CoSe400/NF SEM with different scanning multiples of (a1)W-CoSe200/NF, (b1) W-CoSe300/NF, (c1) W-CoSe400/NF.

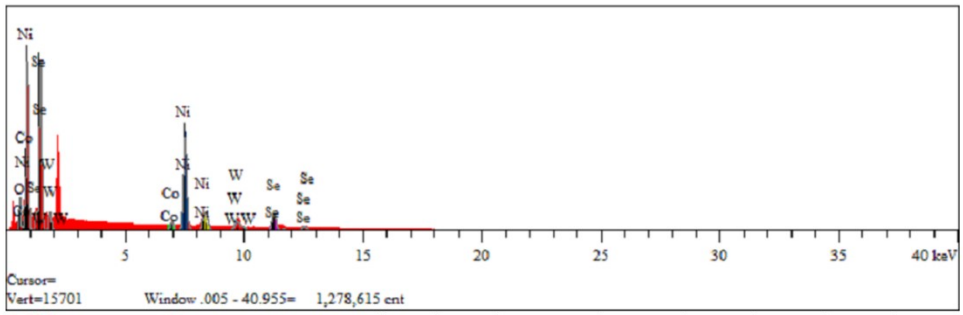

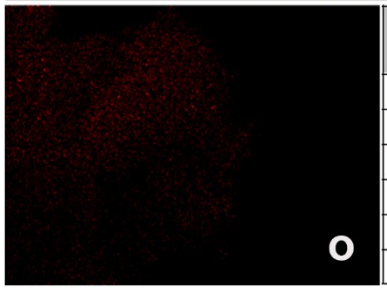

Elt.	Line	Intensity (c/s)	Conc	Units	Error 2-sig	MDL 3-sig	
O	Ka	2,493.47	8.026	wt.%	.166	.200	
Co	Ka	1,097.71	2.561	wt.%	.076	.088	
Ni	Ka	11,445.87	31.057	wt.%	.312	.385	
Se	Ka	2,332.53	32.069	wt.%	.678	.809	
W	La	1,703.25	26.288	wt.%	.658	.792	
			100.000	wt.%			Total

Fig. S2. EDS mapping of W-CoSe300/NF electrocatalyst and corresponding elemental mass percentage content.

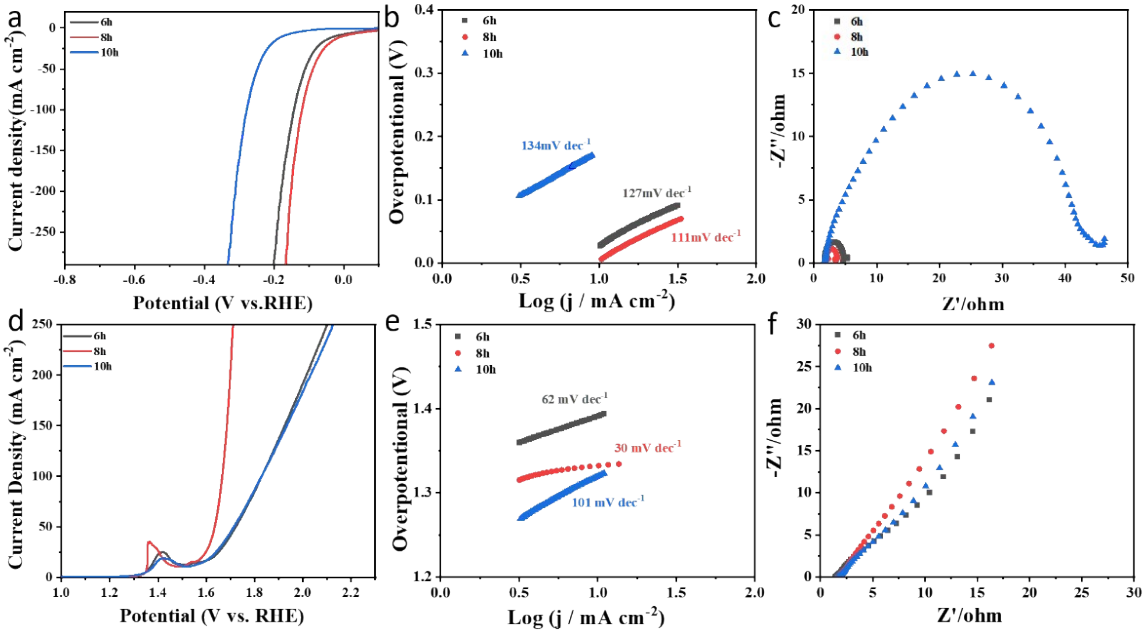

Fig. S3. (a) HER polarization curves (b) Tafel (c) EIS and (d) OER polarization curves (e) Tafel (f) EIS of W-CoO/NF precursors with different reaction times.

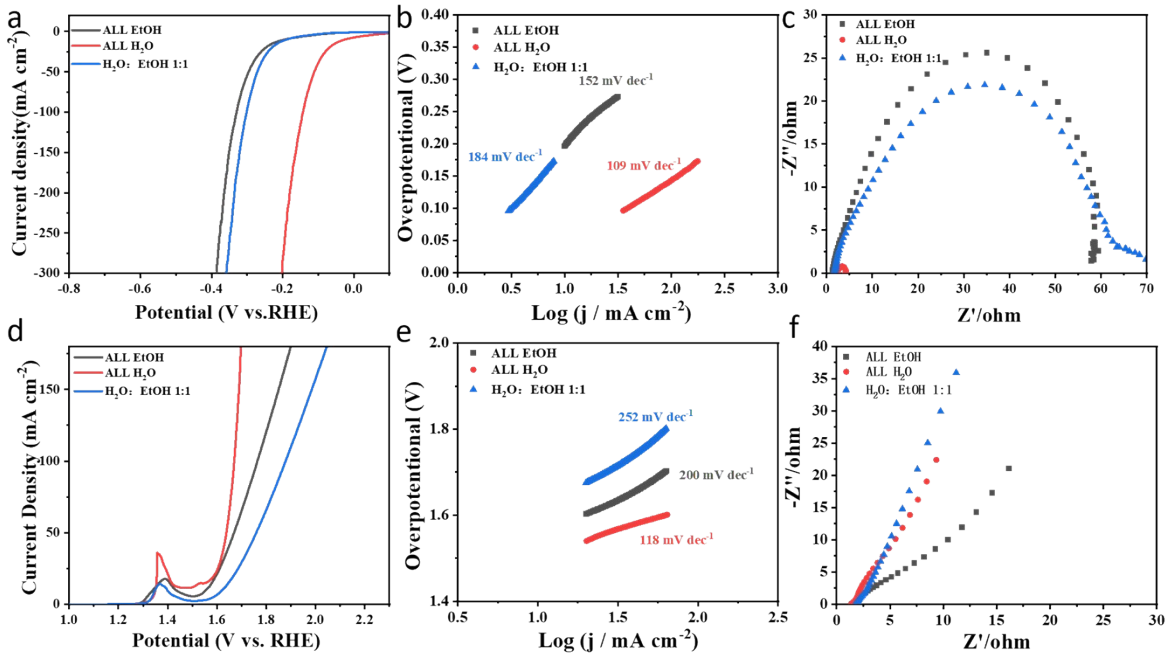

Fig. S4. (a) HER polarization curves (b) Tafel (c) EIS and (d) OER polarization curves (e) Tafel (f) EIS of W-CoO/NF precursors with different solvent ratios.

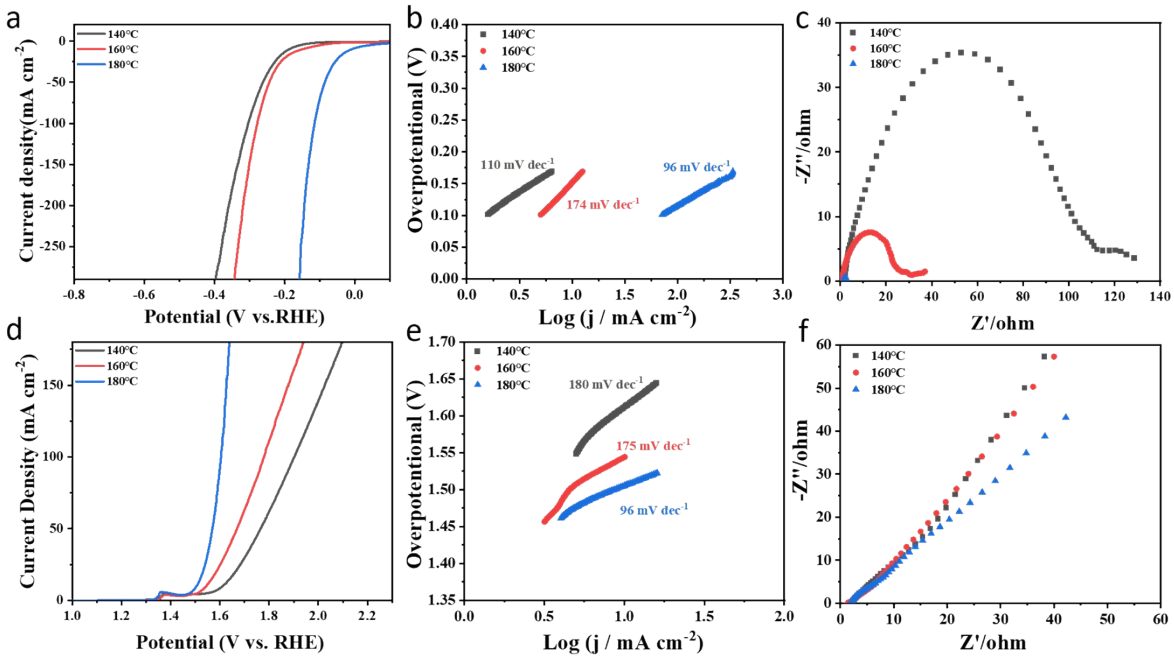

Fig. S5. (a) HER polarization curves (b) Tafel (c) EIS and (d) OER polarization curves (e) Tafel (f) EIS of W-CoO/NF precursors with different reaction temperatures.

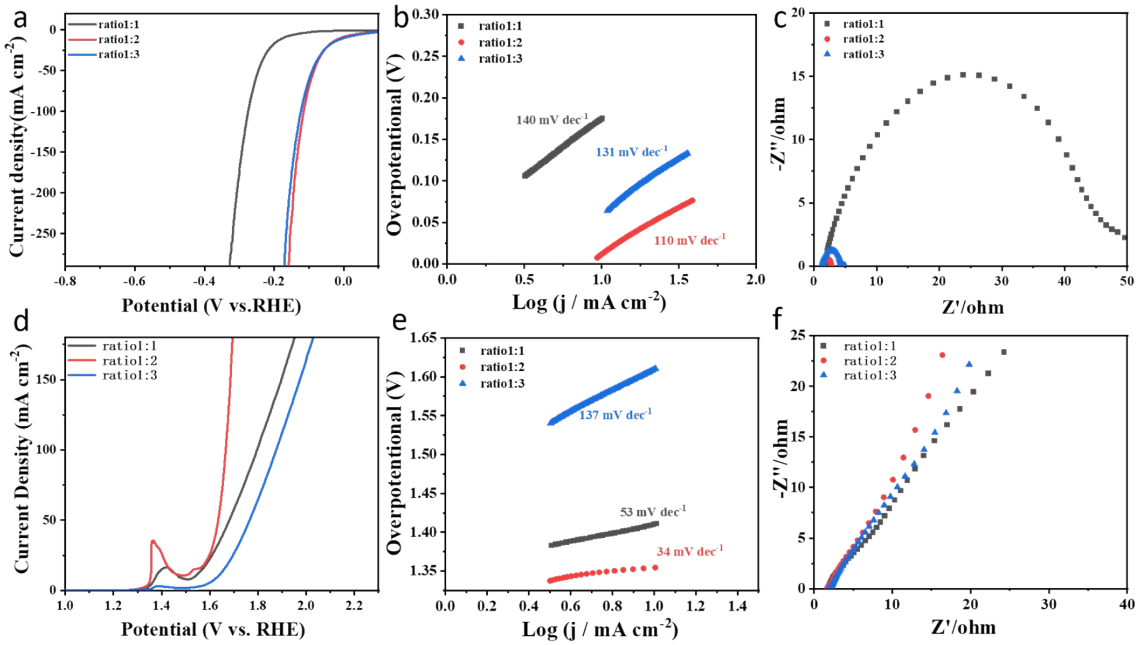

Fig. S6. (a) HER polarization curves (b) Tafel (c) EIS and (d) OER polarization curves (e) Tafel (f) EIS of W-CoO/NF precursors with different reaction solute mass ratio.

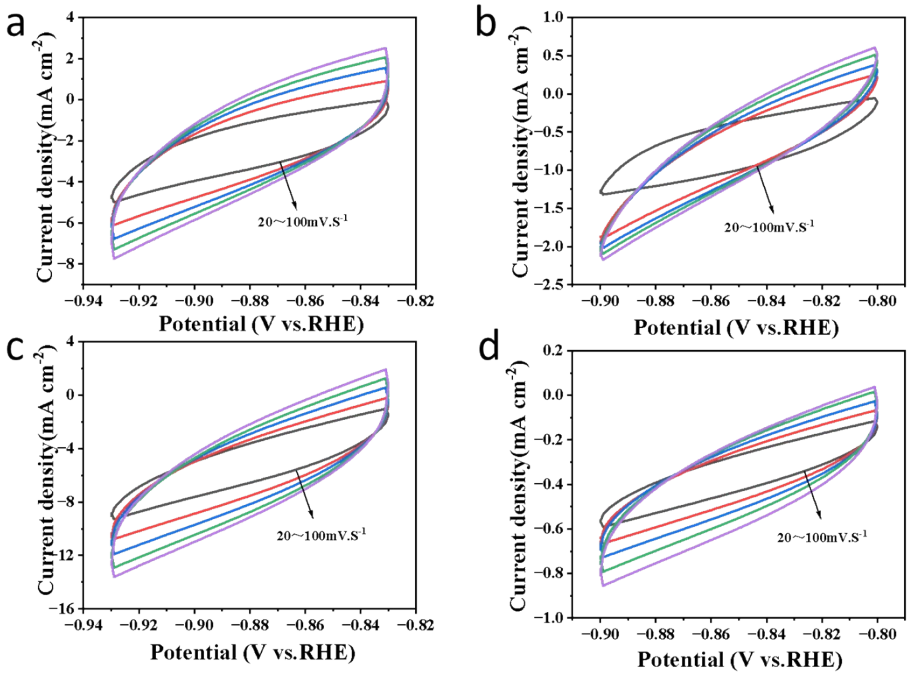

Fig. S7. HER-CV of (a) W-CoO/NF (b) W-CoSe200/NF (c) W-CoSe300/NF and (d) W-CoSe400/NF at different sweep speeds.

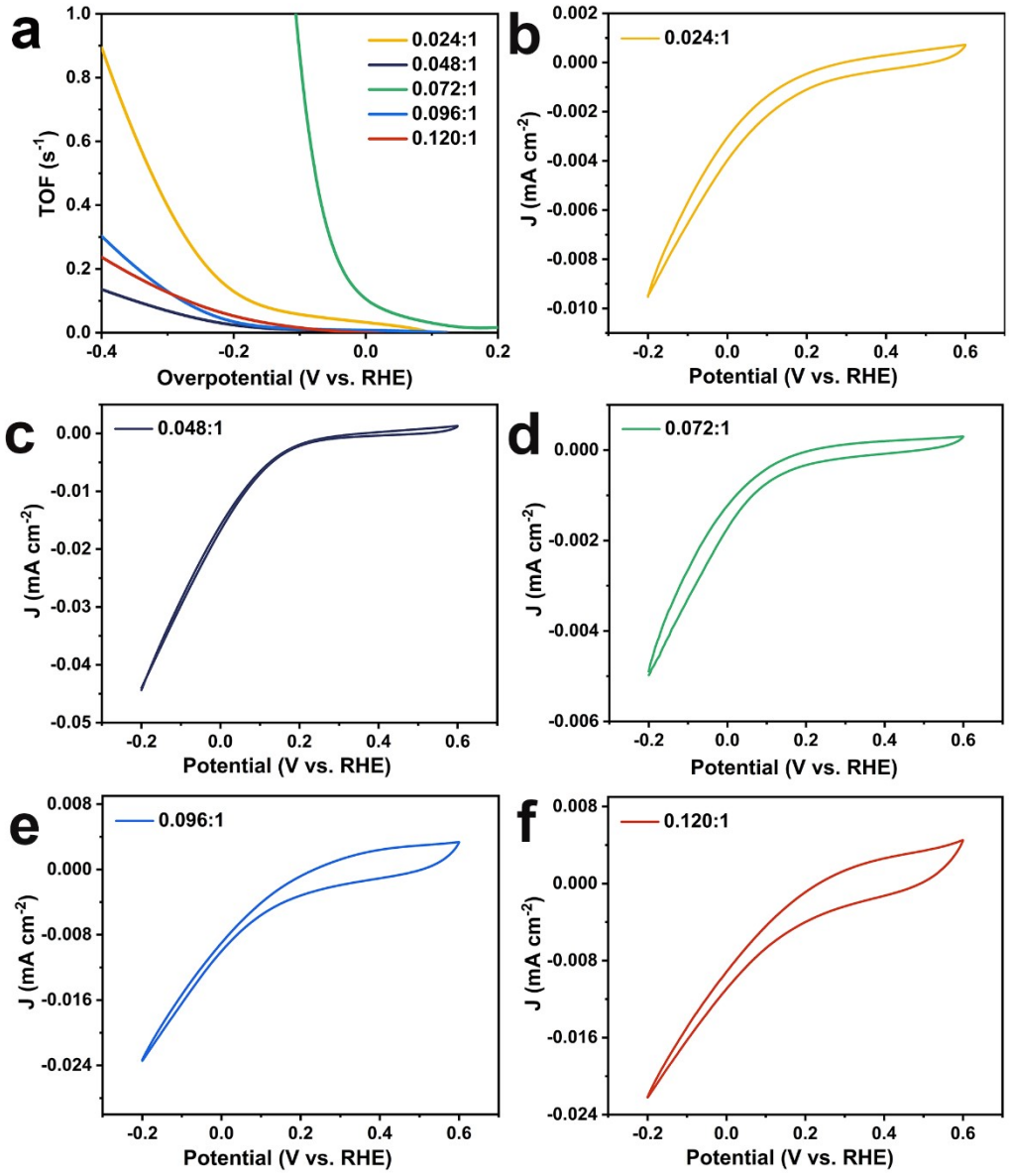

Fig. S8. The turnover frequency (TOF) of W-CoSe300/NF electrocatalysts with different M ($H_3PW_{12}O_{40}$)/M ($C_4H_6CoO_4$) ratios and their corresponding cyclic voltammetry (CV) curves (in PBS solution, pH ≈ 7).

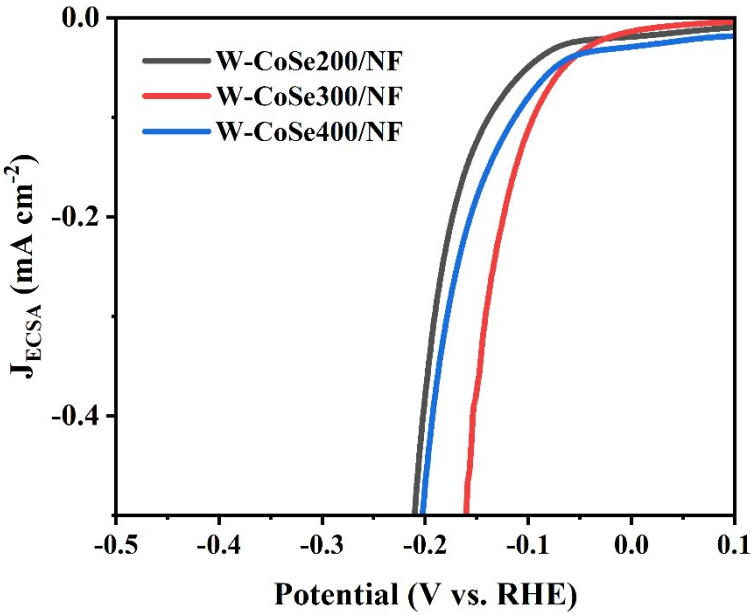

Fig. S9. LSV curves of W-CoSe200/NF, W-CoSe300/NF, and W-CoSe400/NF electrocatalyst normalized by ECSA.

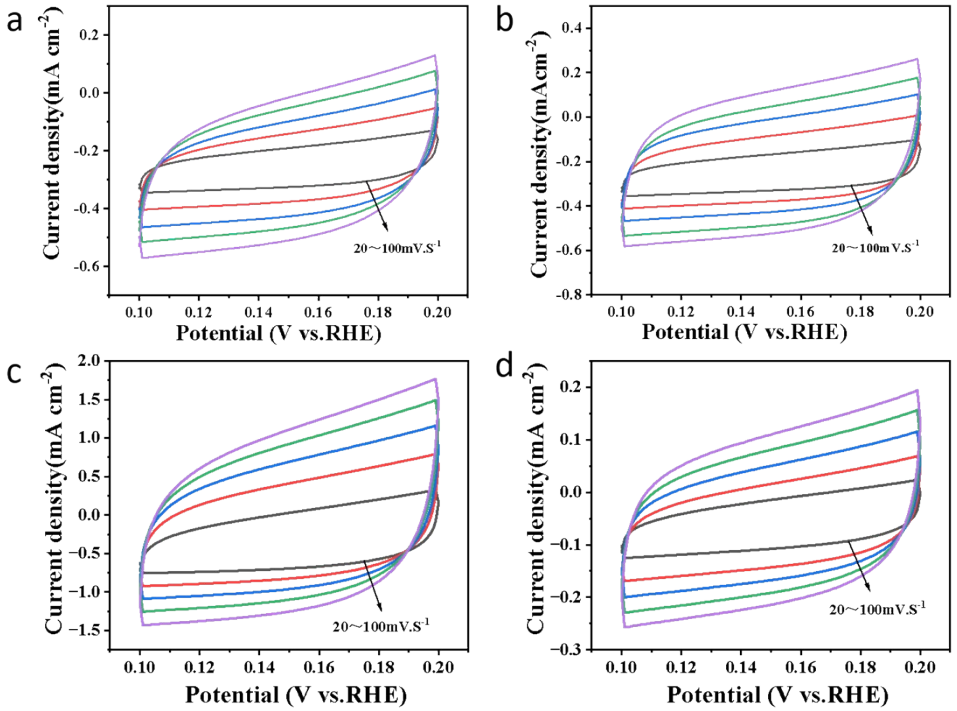

Fig. S10. OER-CV of (a) W-CoO/NF (b) W-CoSe200/NF (c) W-CoSe300/NF and (d) W-CoSe400/NF at different sweep speeds.

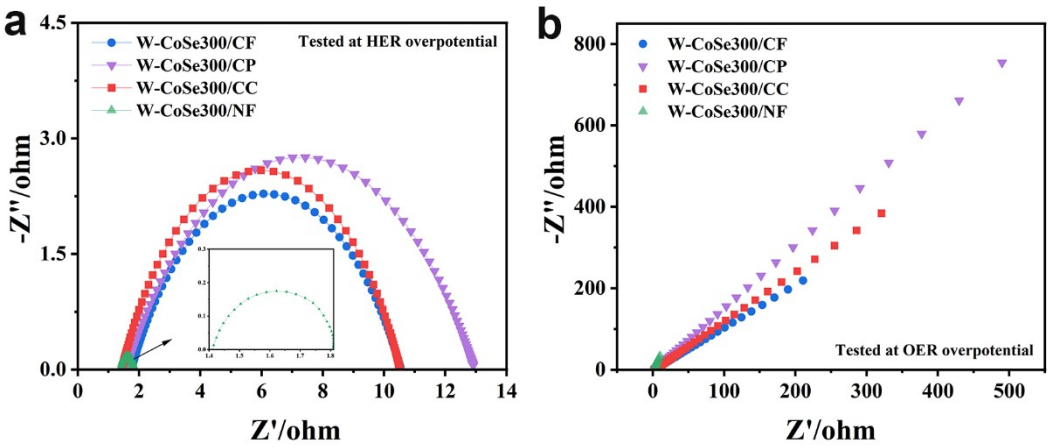

Fig. S11. EIS Nyquist plots of W-CoSe300 electrocatalysts loaded on different conductive substrates.

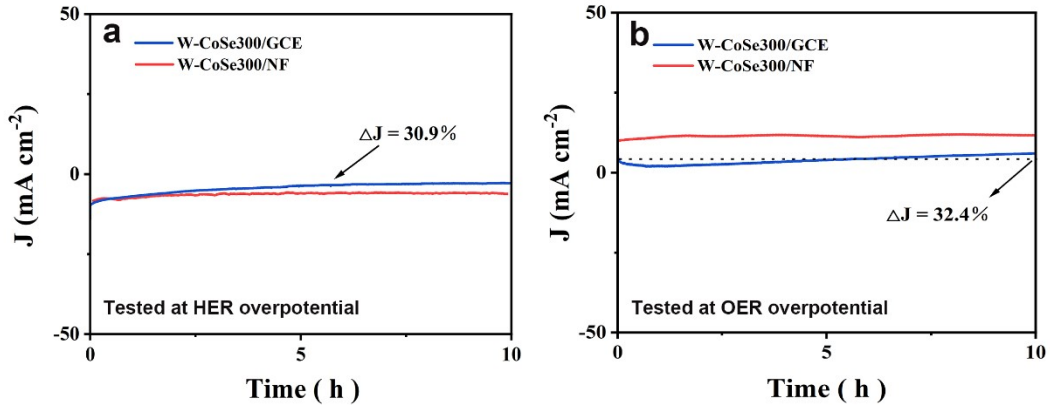

Fig. S12. Stability tests of W-CoSe300/GCE and W-CoSe300/NF electrocatalysts under HER and OER overpotentials (GCE = glassy carbon electrode).

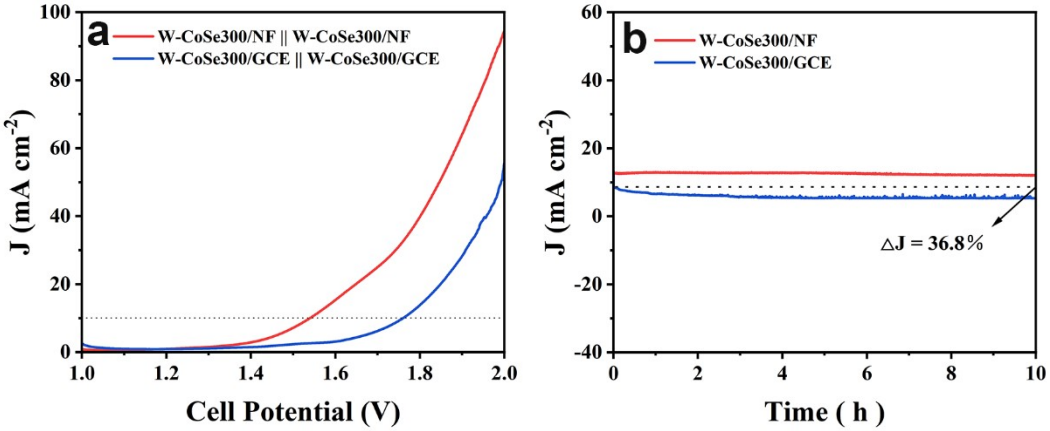

Fig. S13. OWS performance of W-CoSe300/GCE (GCE = glassy carbon electrode) and W-CoSe300/NF electrocatalysts: (a) LSV curves, (b) electrochemical stability test.

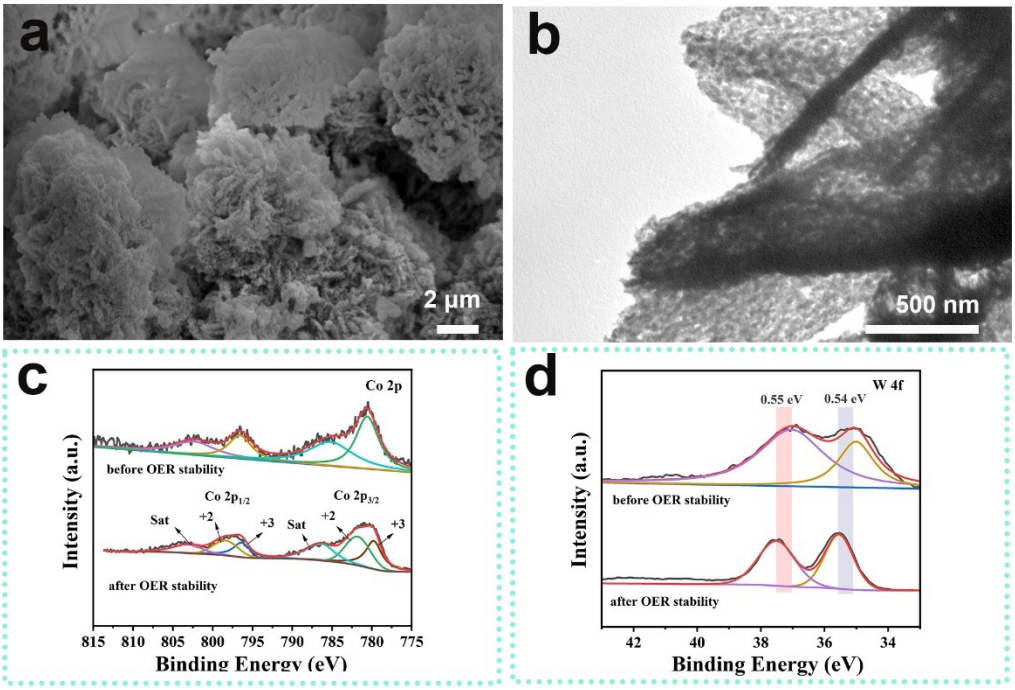

Fig. S14. Characterization analysis of the W-CoSe300/NF electrocatalyst after OER stability testing: (a) SEM image, (b) TEM image, (c, d) XPS spectra.